S. Cacciola, C.E.D. Riboldi
Equalizing Aerodynamic Blade Loads Through Individual Pitch Control via Multiblade Multilag Transformation
Journal of Solar Energy Engineering, Vol. 139, N. 6, 2017, 61008 (8 pages)
doi:10.1115/1.4037744

Equalizing Aerodynamic Blade Loads Through Individual Pitch Control Via Multi–Blade Multi–Lag Transformation

Stefano Cacciola, Ph.D. **Carlo E.D. Riboldi, Ph.D.**
Dept. of Aerospace Science and Technology
Politecnico di Milano
Milano, Italy 20156
Email: {stefano.cacciola, carlo.riboldi}@polimi.it

Control algorithms for rotor load mitigation are today generally adopted by industry. Most of them are based on the Coleman transformation, which is easy to implement and bears satisfactory results when the rotor is balanced. A multitude of causes, e.g. blade erosion, dirt and especially pitch misalignment, may create significant imbalances. This gives birth to undesirable vibrations and reduced control performance in terms of load mitigation. In this paper, an alternative transformation is introduced, able to detect and quantify the rotor load harmonics due to aerodynamic imbalance. Next, a control algorithm, capable of targeting rotor imbalance itself and simultaneously lowering rotor loads, is presented. The effectiveness of the proposed solution is confirmed through simulations in virtual environment.

1 Introduction

The great advantage provided by individual pitch control (IPC) primarily on blade and shaft loads of wind turbines has fueled a relevant research effort towards possible implementations and applications of this control technique, as witnessed by the extensive literature on the topic [1–10].

Among the most widespread IPC techniques for three–bladed wind turbines are those developed by Bossanyi based on the multi–blade (MB) Coleman transformation. The basics of this signal–processing algorithm lie in the idea of obtaining a measurement of the nodding and yawing moment on the cross–section of the shaft by suitably transforming measurements of the out–of–plane bending moments on the blades. The cross sectional loads so obtained can be fed back to two decoupled control loops, resulting in two control signals that, once transformed back via an inverse Coleman transformation, provide three zero–mean pitch signals. Despite the name, Bossanyi's IPC produces a cyclic – i.e. not strictly individual – pitch input, able to reduce both the average of the nodding and yawing moments on the shaft and the harmonic amplitudes of the out–of–plane on the blades corresponding to the frequency of the transformation [2, 11].

As witnessed by many results in the literature, processing and control algorithms based on this transformation are relatively easy to implement and provide satisfactory results [4–6].

Relevant drawbacks of Bossanyi's IPC techniques based on the Coleman transformation are the tendency to overstress actuators and the introduction of spurious load components in presence of blade aerodynamic imbalance – like in presence of pitch misalignment. While the former can be satisfactorily compensated through a balanced tuning of the control gains and of the sections of the wind speed envelope where IPC is activated as shown in [6, 10], the latter is not easy to tackle unless a richer information on the state of the rotor is considered. Being a primary technological issue with a negative effect on loads and posing relevant requirements on control robustness, various methods to detect and treat pitch imbalance have been proposed [12, 13]. In the first, neural networks are considered to only detect the presence of an imbalance, providing information on the severity of the problem and which blade is affected, assuming only one blade misaligned. The second proposes a control algorithm capable of reducing loads induced by blade misalignment. Such algorithm makes use of an extended Coleman transformation whose outputs, averaged over one rotor revolution, can be used as feed-back measurements for rotor imbalance mitigation.

The aim of the present paper is to introduce an alternative to the Coleman transformation, the multi–blade multi–lag (MBML) transformation, which exploiting the same sensor suite required for the usual transformation — including bending loads from all blades (multi–blade) — allows to obtain a richer description of the loads through a smart sampling at specifically selected rotor phase shifts (multi–lag), typically covering much less than one rotor revolution. In this work, firstly the theoretical features and properties of the MBML transformation will be demonstrated and compared to the classic Coleman MB transformation. Afterwards, the ability of the new signal–conditioning algorithm to provide all information for feeding a usual Bossanyi's IPC

control and for simultaneously targeting aerodynamic imbalance will be illustrated. It will be shown how to effectively correct pitch imbalance via a dedicated, strictly individual – i.e. not cyclic – pitch control loop. Moreover, the ensuing disturbance to the underlying collective trimmer is compensated through a further compensating loop, in a multi–layer fashion. Numerical results from the application of the new MBML transformation to the model of an existing testbed will showcase the performance of the proposed signal–conditioning and control algorithm in successfully tackling the effects of aerodynamic imbalance.

2 Multi–Blade Multi–Lag Transformation

2.1 Computation of harmonics using the demodulation and the multi–blade transformation

In steady conditions, the behavior of a three–bladed wind turbine settles in a cyclostationary regime, in which the blade out-of-plane bending moments, $m^{(1)}$, $m^{(2)}$ and $m^{(3)}$, show up as periodic signals shifted by 120 degrees as

$$\begin{aligned} m^{(1)}(\psi) &= a_0 + \sum_n a_{n_c}\cos(n\psi_1) + a_{n_s}\sin(n\psi_1) \\ m^{(2)}(\psi) &= a_0 + \sum_n a_{n_c}\cos(n\psi_2) + a_{n_s}\sin(n\psi_2) \\ m^{(3)}(\psi) &= a_0 + \sum_n a_{n_c}\cos(n\psi_3) + a_{n_s}\sin(n\psi_3), \end{aligned} \tag{1}$$

where ψ is the rotor azimuth, ψ_i is the azimuth angle of the ith blade, such that $\psi_1 = \psi$, $\psi_2 = \psi + 2\pi/3$ and $\psi_3 = \psi + 4\pi/3$, and finally a_0 represents the constant, or $0\times$Rev, harmonic while a_{n_c} and a_{n_s} the cosine and sine amplitude of the $n\times$Rev.

The harmonic amplitudes, collected for simplicity in the vector $\boldsymbol{a} = \{a_0, a_{1_c}, a_{1_s}, a_{2_c}, a_{2_s}, \ldots\}^T$, can be extracted by demodulating the signal of one of the moments. Accordingly, one has to consider multiple samples of the signal and of the azimuth, noted respectively m_k and ψ_k, $k = 1, \ldots, N$, where N is the total number of samples, and stack them in two column vectors $\boldsymbol{m}_{\text{smp}}$ and $\boldsymbol{\psi}_{\text{smp}}$. Defining the regressor matrix $\boldsymbol{X} = \left[\mathbf{1}, \cos(\boldsymbol{\psi}_{\text{smp}}), \sin(\boldsymbol{\psi}_{\text{smp}}), \cos(2\boldsymbol{\psi}_{\text{smp}}), \sin(2\boldsymbol{\psi}_{\text{smp}}), \ldots\right]$, being $\mathbf{1}$ the unitary regressor, the least square estimate of $\boldsymbol{a}$, noted $\boldsymbol{a}_{\text{E}}$, is given by $\boldsymbol{a}_{\text{E}} = (\boldsymbol{X}^T\boldsymbol{X})^{-1}\boldsymbol{X}^T\boldsymbol{m}_{\text{smp}}$.

The major advantage of the demodulation is that the regressors, i.e. the columns of matrix $\boldsymbol{X}$, become orthogonal vectors when an integer multiple of the rotor period is used as projection window. This leads to the rejection of all harmonics present in the signal except those considered for the demodulation. The cost one has to pay is that this algorithm needs to look in the past for at least one rotor revolution and consequently suffers from a significant memory effect, which renders the harmonic estimation lagged and therefore not suitable for control applications especially in highly dynamical scenarios [5].

Another common and widely used approach to extract the 0 and $1\times$Rev amplitudes from three blade signals is the Coleman or multi–blade transformation (MB),

$$\boldsymbol{a}_{1\text{E}} = \boldsymbol{C}(\psi)\boldsymbol{m}(\psi), \tag{2}$$

where $\boldsymbol{a}_{1\text{E}} = \{a_0, a_{1_c}, a_{1_s}\}^T_{\text{E}}$, $\boldsymbol{m}(\psi) = \{m^{(1)}(\psi), m^{(2)}(\psi), m^{(3)}(\psi)\}$ and the MB transformation matrix is

$$\boldsymbol{C}(\psi) = \frac{2}{3}\begin{bmatrix} 1/2 & 1/2 & 1/2 \\ \cos(\psi_1) & \cos(\psi_2) & \cos(\psi_3) \\ \sin(\psi_1) & \sin(\psi_2) & \sin(\psi_3) \end{bmatrix}. \tag{3}$$

The inverse of the MB transformation matrix, useful to work out $\boldsymbol{m}$ given the amplitudes $\boldsymbol{a}_1 = \{a_0, a_{1_c}, a_{1_s}\}$, is

$$\boldsymbol{Q} = \begin{bmatrix} 1 & \cos(\psi_1) & \sin(\psi_1) \\ 1 & \cos(\psi_2) & \sin(\psi_2) \\ 1 & \cos(\psi_3) & \sin(\psi_3) \end{bmatrix}. \tag{4}$$

The main advantage of the MB transformation lies in its ability to extract the harmonic amplitudes by exploiting three 120 degree shifted signals, in this case the blade loads, without the need of sampling measures over one rotor revolution. This fact renders the MB transformation more suited to generating feed–back signals for control purposes in highly turbulent conditions, as proven by its widespread adoption by industry.

The drawbacks of the MB transformation are mainly two. Firstly, the harmonics extracted result to be polluted by frequencies equal to multiples of the number of blades (i.e. $3\times$Rev, $6\times$Rev, …), which should be canceled by using a low–pass filter. Secondarily, in the case one or more blades are misaligned from the reference pitch setting, also other harmonics, $1\times$Rev, $2\times$Rev, …, are present significantly in the output of the MB transformation. This additional load components are not usually canceled by the filter generally adopted for cutting off frequencies higher than $3\times$Rev. Consequently, such harmonics entail a control action at unwanted frequencies, increasing the pitch actuator duty cycle (ADC) with respect to the same controlled working with a balanced, i.e. not misaligned, rotor. It is interesting to notice that this latter problem could be easily digested if the harmonic amplitudes were extracted using the standard demodulation.

This discussion highlights the fact that there are two opposite needs. The first is being fast in demodulating the harmonics to provide good feed–back measurements. From this point of view, the MB transformation represents the best possible choice. The second is to have a good rejection of polluting harmonics, which may entail a spill–over of control action. Now, the demodulation fulfills this target best.

However, it is clear that none of them may represent the optimal solution for both needs and that a better trade–off is to be derived.

2.2 Definition of the Multi–Blade Multi–Lag Transformation

The multi–blade multi–lag (MBML) concept defines a family of transformations which use multiple samples of all blade loads in order to extract the harmonic amplitude of rotor signals. The clear advantage of MBML is to have more pieces of information to be exploited than the standard MB transformation. On the other hand, it may require less memory than a demodulation.

A MBML transformation is indicated with $\mathcal{C}^B_{L,\Delta\psi}$, where B is the number of blades, L is the number of lags and $\Delta\psi$ is the phase shift of each lag. As an example, the transformation $\mathcal{C}^3_{1,\pi/3}$ uses the loads of 3 blades, sampled at the current time instant and with a lag of 60 degrees. Hereafter, unless explicitly indicated, only three–bladed rotors will be considered and the suffix B will be dropped from the indication of the MBML transformation, not to clutter the notation.

Figure 1 shows, for three–bladed rotors, the azimuthal positions needed by a generic MBML transformation $\mathcal{C}_{L,\Delta\psi}$, on the left, by $\mathcal{C}_{1,\pi/3}$, in the center, and by $\mathcal{C}_{2,2\pi/9}$, on the left.

Clearly, within this framework, the standard Coleman transformation is viewed as a MBML $\mathcal{C}_0$ as no lags are required, whereas the demodulation is $\mathcal{C}^1_{N-1,2\pi/N}$, being N the total number of samples in a rotor revolution.

The value $s = L\Delta\psi$ is called *support* of the transformation and it can be considered as a measure of how long the transformation needs to look in the past. The smaller the support, the faster the transformation.

It is self–evident that a transformation with a support of a rotor revolution is useless as it does not entail any additional improvement with respect to the standard demodulation.

In terms of applications, the enlarged informative content of the MBML transformation can be used for several purposes, such as:

1. Computation of aerodynamic imbalances, e.g. those induced by pitch misalignment, with application to equalization of blade pitch settings.
2. Simultaneous extraction of specific harmonics and rejection of others up to a specific multiple of the rotor frequency.
3. Fast demodulation of blade load signal for two–bladed rotors with application to the related individual pitch control.
4. Blade load peak shaving.

In this paper, point 1 will be extensively addressed, for the aerodynamic imbalance represents currently one of the major problems for large and very large wind turbines. Point 2 will be described in an appendix A. Finally, points 3 and 4 will be part of forthcoming publications.

3 Measuring and Equalizing Pitch Imbalances using the MBML Transformation

Consider now an unbalanced rotor in which the blade pitch settings are different. The out-of-plane bending moment of the three blades will be no more identical and shifted even in steady conditions, for the pitch offset has introduced, among the others, a prominent constant bias between blade load values.

Under these assumptions, the out-of-plane loads can be expanded as

$$\begin{aligned} m^{(1)}(\psi) &= a_0 + b_1 + \sum_n a_{n_c}\cos(n\psi_1) + a_{n_s}\sin(n\psi_1) \\ m^{(2)}(\psi) &= a_0 + b_2 + \sum_n a_{n_c}\cos(n\psi_2) + a_{n_s}\sin(n\psi_2), \\ m^{(3)}(\psi) &= a_0 + b_3 + \sum_n a_{n_c}\cos(n\psi_3) + a_{n_s}\sin(n\psi_3) \end{aligned} \tag{5}$$

where b_1, b_2 and b_3 corresponds to the misalignment–induced offsets.

With the aim of extracting the constant term, a_0, the $1\times$Rev amplitudes, a_{1_c} and a_{1_s}, and the three biases, b_1, b_2 and b_3, one has to consider at least six pieces of information. Under the umbrella of the MBML concept, this corresponds to the use of a transformation with $L = 1$ and $\Delta\psi$ to be defined. To this end, the blade moments at the rotor azimuth ψ and at a lagged position $\psi - \Delta\psi$ can be written in a compact form as

$$\begin{Bmatrix} \boldsymbol{m}(\psi) \\ \boldsymbol{m}(\psi-\Delta\psi) \end{Bmatrix} = \begin{bmatrix} \boldsymbol{Q}(\psi) & \boldsymbol{I} \\ \boldsymbol{Q}(\psi-\Delta\psi) & \boldsymbol{I} \end{bmatrix} \begin{Bmatrix} \boldsymbol{a}_1 \\ \boldsymbol{b} \end{Bmatrix} + \boldsymbol{f}, \tag{6}$$

where $\boldsymbol{I}$ is the identity matrix of suitable dimensions, $a_1 = \{a_0, a_{1_c}, a_{1_s}\}$, $\boldsymbol{b} = \{b_1, b_2, b_3\}^T$ and $\boldsymbol{f}$ represents the contribution of harmonics higher than $1\times$ Rev.

Clearly, Eq. 6 cannot be inverted so as to estimate $\boldsymbol{a}_1$ and $\boldsymbol{b}$ out of $\boldsymbol{m}$, as the sum of the last three columns of the to-be-inverted matrix is exactly equal to the first one. Notice that the ill-posedness of the problem will stay the same despite the number of blades, lags and azimuthal sampling. This fact is not surprising because, from a physical standpoint, the mean value of the biases, $b_{\text{col}} = (b_1 + b_2 + b_3)/3$, hereafter called *collective offset*, cannot be formally distinguished by the constant amplitude of the loads a_0.

The impact of this on a practical side is that estimating three biases simultaneously, and in turn the collective offset, is impossible unless one provides the problem with a complementary information to the measures of the blade loads.

To this end, one has to remove the indeterminacy of the collective offset. This issue is solved by appending an extra condition to system (6) so as to constrain the collective offset to 0. This may lead to a small bias in the collective pitch angle after the three blade pitches are equalized, which should be compensated. At first, the equalizing algorithm will be considered, then the collective offset compensation will be addressed.

With the addition of the constraint, problem (6) is rewritten as

$$\begin{Bmatrix} \boldsymbol{m}(\psi) \\ \boldsymbol{m}(\psi-\Delta\psi) \\ 0 \end{Bmatrix} = \begin{bmatrix} \boldsymbol{Q}(\psi) & \boldsymbol{I} \\ \boldsymbol{Q}(\psi-\Delta\psi) & \boldsymbol{I} \\ \boldsymbol{0} & \boldsymbol{1} \end{bmatrix} \begin{Bmatrix} \boldsymbol{a}_1 \\ \boldsymbol{b} \end{Bmatrix} + \boldsymbol{f}, \tag{7}$$

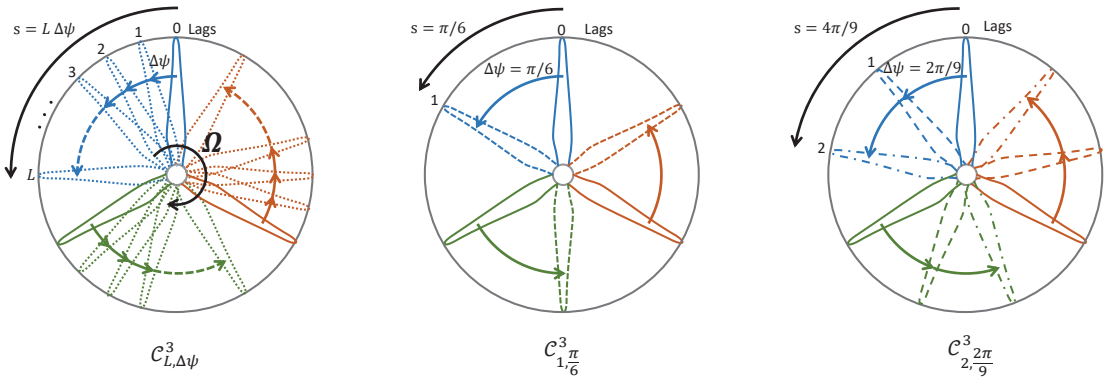

Figure 1. Rotor positions for a generic MBML transformation, left, for $\mathcal{C}^3_{1,\pi/3}$, center, and $\mathcal{C}^3_{2,2\pi/9}$, right.

where $\mathbf{0} = \{0, 0, 0\}$ and $\mathbf{1} = \{1, 1, 1\}$.

For $\Delta\psi = 2\pi/3$, Eq. (7) can be pseudo-inverted yielding the estimation of harmonics and biases

$$\begin{Bmatrix} \boldsymbol{a}_1 \\ \boldsymbol{b} \end{Bmatrix}_{\mathrm{E}} = \begin{bmatrix} \boldsymbol{T}\boldsymbol{C}(\psi+\frac{\pi}{6}) & \boldsymbol{T}\boldsymbol{C}(\psi-\frac{2\pi}{3}-\frac{\pi}{6}) \\ \boldsymbol{B} & \boldsymbol{B}^T \end{bmatrix} \begin{Bmatrix} \boldsymbol{m}(\psi) \\ \boldsymbol{m}(\psi-\frac{2\pi}{3}) \end{Bmatrix}, \quad (8)$$

where

$$\boldsymbol{B} = \begin{bmatrix} 1/3 & 0 & -1/3 \\ -1/3 & 1/3 & 0 \\ 0 & -1/3 & 1/3 \end{bmatrix} \quad (9)$$

and $\boldsymbol{T} = \mathrm{diag}(1/2, \tan(\pi/6), \tan(\pi/6))$.

It is possible to show that this transformation, if fed with three misaligned signals as in Eq. (5), returns the following output

$$\begin{aligned} a_{0\mathrm{E}} &= a_0 + b_{\mathrm{col}} + O(3\times\mathrm{Rev}) \\ a_{1_{\mathrm{c}}\mathrm{E}} &= a_{1_{\mathrm{c}}} + O(3\times\mathrm{Rev}) \\ a_{1_{\mathrm{s}}\mathrm{E}} &= a_{1_{\mathrm{s}}} + O(3\times\mathrm{Rev}) \\ b_{w\mathrm{E}} &= b_w - b_{\mathrm{col}}, \quad w = 1,2,3, \end{aligned} \quad (10)$$

where $O(3\times\mathrm{Rev})$ indicates a polluting error at frequencies multiple of the number of blades ($3\times$Rev, $6\times$Rev,...), similarly to the standard MB transformation.

From the estimated amplitudes, Eq. (10), a new control scheme, consisting of three parallel loops, can be employed in addition to the standard trimmer, which produces a collective pitch input, β_{col}, and the electrical torque.

In the first loop, called *cyclic control*, signals $a_{1_{\mathrm{c}}\mathrm{E}}$ and $a_{1_{\mathrm{s}}\mathrm{E}}$, filtered to remove the residual $3\times$Rev component, can be used as feed–back measurements in a $1\times$Rev load reduction control algorithm identical to the standard Bossanyi's IPC [1, 2],

$$\boldsymbol{\beta}^{\mathrm{cyc}} = \tilde{\boldsymbol{C}}_{\mathrm{MB}}(\psi)\left(k_{\mathrm{P}}^{\mathrm{cyc}}\boldsymbol{I}\boldsymbol{a}_{\mathrm{cyc}} + k_{\mathrm{I}}^{\mathrm{cyc}}\boldsymbol{I}\int\boldsymbol{a}_{\mathrm{cyc}} + k_{\mathrm{D}}^{\mathrm{cyc}}\boldsymbol{I}\dot{\boldsymbol{a}}_{\mathrm{cyc}}\right), \quad (11)$$

where $\boldsymbol{\beta}^{\mathrm{cyc}}$ is the cyclic pitch input, $\boldsymbol{a}_{\mathrm{cyc}} = \{a_{1_{\mathrm{c}}\mathrm{E}}, a_{1_{\mathrm{s}}\mathrm{E}}\}^T$, $\tilde{\boldsymbol{C}}_{MB}$ is the anti MB transformation

$$\tilde{\boldsymbol{C}}_{MB} = \begin{bmatrix} \cos(\psi_1) & \cos(\psi_2) & \cos(\psi_3) \\ \sin(\psi_1) & \sin(\psi_2) & \sin(\psi_3) \end{bmatrix}^T \quad (12)$$

and $k_{\mathrm{P}}^{\mathrm{cyc}}$, $k_{\mathrm{I}}^{\mathrm{cyc}}$ and $k_{\mathrm{D}}^{\mathrm{cyc}}$ are respectively the proportional, integral and derivative gains of the cyclic control. Those gains are to be tuned similarly to the usual Bossanyi's IPC, as the meaning of the feed–back quantity, $\boldsymbol{a}_{\mathrm{cyc}}$, is the same.

A second loop, called *equalizing control*, can employ the biases $b_{w\mathrm{E}}$ to equalize the pitch settings so as to mitigate the rotor aerodynamic imbalance. For each $b_{w\mathrm{E}}$, a straightforward PID control can be used to compute the equalizing pitch control signal $\Delta\beta_w$ as

$$\Delta\beta_w = k_{\mathrm{P}}^{\mathrm{eql}} b_{w\mathrm{E}} + k_{\mathrm{I}}^{\mathrm{eql}}\int b_{w\mathrm{E}} + k_{\mathrm{D}}^{\mathrm{eql}}\dot{b}_{w_{\mathrm{E}}}, \quad (13)$$

where $k_{\mathrm{P}}^{\mathrm{eql}}$, $k_{\mathrm{I}}^{\mathrm{eql}}$ and $k_{\mathrm{D}}^{\mathrm{eql}}$ are now the gains of the equalizing control. A good control action can be obtained already with only a hand–tuned integral control component. With this second loop, the standard Bossanyi's IPC, based on a zero–mean cyclic pitch motion, is outperformed since now the blade pitches are allowed to move individually. Notice now the effect of the constraint added in Eq. (7). Being the collective offset b_{col} not present in the estimation of the biases — see Eq. (10) — it is only possible to equalize the blade pitches, leaving the collective misalignment unchanged. This fact is far from being a problem because first collective misalignment is expected to be low in real operations and, secondarily, it can be compensated with a third control loop, as described in the following.

In the third loop, the *collective compensating control*, quantity b_{col} is compensated by taking advantage of a reference collective out–of–plane bending moment

$$a_{0\mathrm{REF}} = \frac{1}{2}\rho V^2 R C_m(\lambda, \beta, V), \quad (14)$$

where V is the wind speed, R the rotor radius, λ the tip-speed-ratio, β the collective pitch setting and $C_m(\lambda,\beta,V)$ the non-dimensional cone coefficient, introduced in [23]. For each instant of time, given the measurements of λ, β, V and ρ, and a look–up table describing the cone coefficient, one is able to compute the expected out–of–plane collective load with (14). Since for null collective offset $a_{0\mathrm{E}}$ should be equal to $a_{0\mathrm{REF}}$, the difference $y = a_{0\mathrm{E}} - a_{0\mathrm{REF}}$ can be fed back by a standard PID control to compensate the collective pitch offset. The compensating action is formalized as

$$\Delta\beta_{\mathrm{col}} = k_{\mathrm{P}}^{\mathrm{cmc}} y + k_{\mathrm{I}}^{\mathrm{cmc}} \int y + k_{\mathrm{D}}^{\mathrm{cmc}} \dot{y}, \tag{15}$$

where $k_{\mathrm{P}}^{\mathrm{cmc}}$, $k_{\mathrm{I}}^{\mathrm{cmc}}$ and $k_{\mathrm{D}}^{\mathrm{cmc}}$ are now the gains of the collective misalignment compensator. These gains should be tuned carefully to avoid an excessive control action.

It is important to notice that this additional compensation loop is to be triggered only in region II, where the trimmer does not use the pitch to control the machine. In region II-$\frac{1}{2}$ and III, the trimming action is also effective in compensating for possible collective pitch offsets. In order to avoid bumpiness in the response, the switching logic can be smoothed implementing a linear ramp function of the wind speed for the trigger.

Figure 2 summarizes the final control architecture.

4 Results

The results presented in this section have been obtained working in virtual environment with the FAST simulator [19], considering the model of an existing 3.0 MW three–bladed horizontal–axis wind turbine. This model was previously validated with respect to more sophisticated models of the same turbine in different multibody codes. All flexible DOFs of the blades and tower allowed by the FAST simulator have been enabled. The simulator has been coupled with a master dynamically linked library, implementing basic supervisory and trimming control routines, itself linked in a modular fashion to further libraries for signal processing – including an implementation of the MBML transformation – and control – including an individual pitch control logic for load mitigation and/or unbalance equalization, and a controller for compensating collective pitch.

Two features showcasing the usefulness of the MBML tranformation will be presented. Firstly, the use of the MBML–transformed signals to effectively equalize pitch unbalance will be investigated. Secondarily, the ability of a controller based on the MBML transformation to balance out pitch setting inequalities, while also mitigating loads via a dedicated control layer, will be shown. For both scenarios of interest, the MBML transformation defined in Eq. (8) and the related multi–layer control have been used.

In order to provide a detailed picture of the results which can be obtained from the use of the MBML transformation, both a normal wind profile (NWP) and a Category A (Cat. A) turbulent wind scenario defined by the international standards [18] have been considered. In all simulations the machine is kept trimmed through a standard wind–scheduled LQR trimmer [11, 15], governing collective pitch and torque inputs.

4.1 MBML transformation and pitch misalignment equalization

In this scenario the MBML transformation is used to detect pitch imbalance. Based on the use of the extended matrix presented in Eq. (10), the results of detection are transformed loads and values of individual pitch controls necessary for equalizing pitch inequalities. No cyclic pitch control for load mitigation is applied in this scenario.

Since, the control solution in terms of individual pitch does not guarantee null average of the three pitch values for equalization, in partial power region an additional trim compensator has been implemented, as described in Sec. 3. This control layer automatically disengages in full power region. The control input from the compensator is a collective pitch command, computed with a PID control law, suitably tuned to avoid any interference with the underlying trimmer.

Considering Fig. 2, the equalizer and compensator loops are here active, whereas the cyclic control loop is not.

Figure 3 presents a comparison of the time histories of nodding and yawing moments in NWP [18] in partial and full power operational regions (7 m/s (a) and 15 m/s (b) respectively). On both plots in Fig. 3 are reported the results corresponding to a reference condition with no pitch imbalance (green solid), a condition with pitch imbalance with no compensation (yellow dashed) and a third condition where the pitch imbalance is equalized by means of a dedicated individual pitch control loop based on measurements from the MBML transformation (purple dash–dotted). The imbalance has been set to 2 deg, 0.5 deg and -0.5 deg respectively for the three blades. This is substantial if compared to the standard requirement, and with a non–null mean over the three blades. In order to highlight the detrimental effect of pitch imbalance and the effectiveness of equalization, the capability of the simulator have been exploited making the inequality appear at a given time, and activating the equalizer (and compensator, in partial power region) in a later stage.

A further difference between the two plots in Fig. 3 is the action of the compensator in partial power region (plot (a)), whereas in full power region (plot (b)) the trimming controller effectively compensates for the error in collective pitch ensuing from the application of individual pitch control for equalization, so that the collective pitch compensator is not necessary.

From the plots in Fig. 3 the effect of pitch inequality is clearly noticeable, resulting in a severe increase in the $1\times$ Rev oscillations of the two considered load signals as soon as the inequality is imposed (between revolution 6 and 8 at 7 m/s and revolution 8 and 10 at 15 m/s). The activation of the pitch equalizer based on the MBML transformation, soon after round 10 at 7 m/s and 12 at 15 m/s, translates into a remarkable effect on loads, bringing the corresponding signals back to the undisturbed condition.

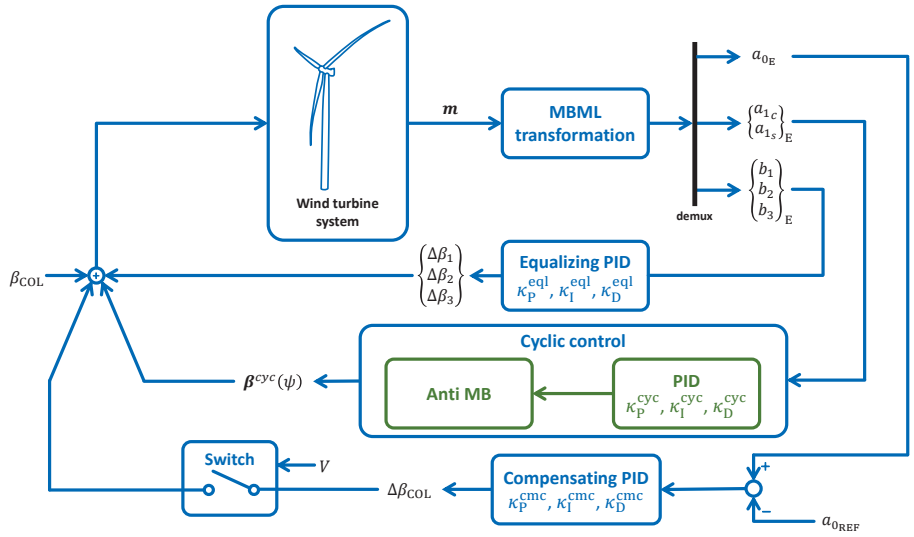

Figure 2. Cyclic, equalizing and collective misalignment compensating control scheme

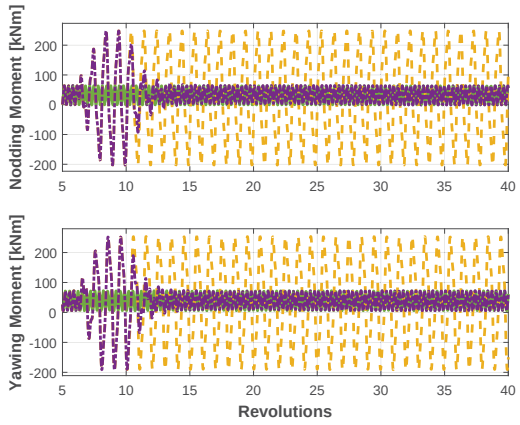

(a)

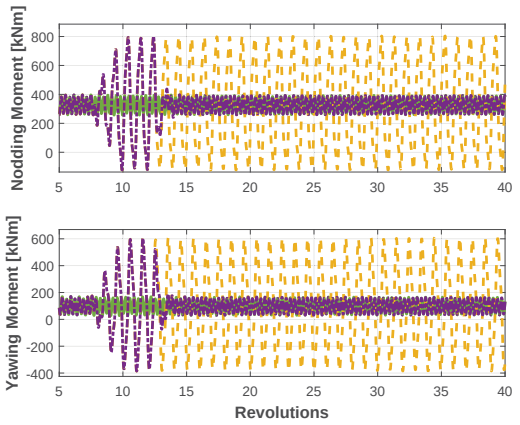

(b)

Figure 3. Comparison of nodding and yawing moments in NWP conditions. (a) 7 m/sec, (b) 15 m/sec. Green solid: no pitch imbalance. Yellow dashed: pitch imbalance, only trimmer. Purple dash–dotted: pitch imbalance, trimmer, MBML–based equalizer.

Figure 4 shows the time histories of the three measured pitches. The signals on the plot include the value of the misalignment, so that a clear distinction can be made between the reference and the disturbed case. Considering the third case, where the pitch command from the controller fed with the output of the MBML transformation is activated, it is possible to see how the pitch control is equalized very precisely, basically canceling out all inequalities. The longer time necessary for the complete equalization of pitch in partial power region (plot (a)) reflects the dynamics of the PID compensator, which is not present in full power region (plot (b)). Another visible advantage provided by MBML–based control, clearly noticeable in Fig. 4(b), is the reduced ADC. This is caused by rotor imbalance introducing $1 \times$ Rev oscillations in the non–rotating parts of the machine and in both rotor speed and aerodynamic torque signals. The trimming control reacts to this harmonic components with an unwanted input at the same frequency.

Similarly good results can be obtained in turbulent wind conditions. Figure 5 refers to 600 sec simulations in Cat. A turbulence with an average speed of 7 m/sec and 15 m/sec ((a) and (b) respectively). Looking at the spectra of yawing and nodding it is possible to notice that the intensity of the $1 \times$ Rev is greatly increased by the effect of pitch imbalance. Similarly to the constant wind case, the activation of the pitch equalizer, and of the compensator in partial power region, pushes the load signals back to the undisturbed condition.

4.2 Pitch misalignment equalization and load mitigation

Among the limitations of Bossanyi's cyclic control for load mitigation there is the inability to effectively work in presence of an undetected pitch imbalance.

The use of the MBML transformation allows to detect

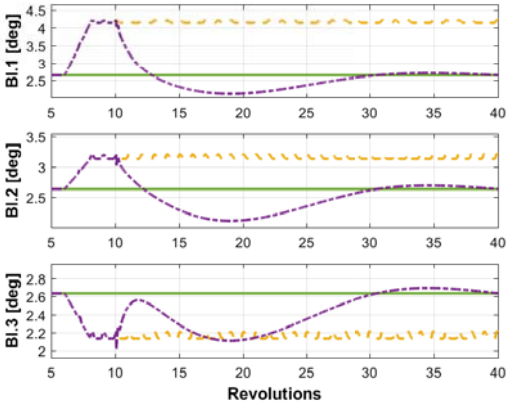

(a)

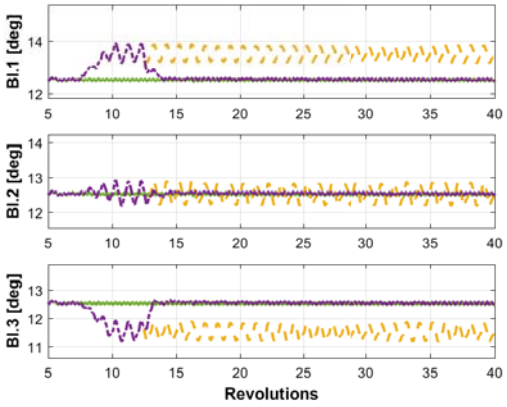

(b)

Figure 4. Comparison of blade pitch in NWP conditions. (a) 7 m/s, (b) 15 m/s. Green solid: no pitch imbalance. Yellow dashed: pitch imbalance, only trimmer. Purple dash–dotted: pitch imbalance, trimmer, MBML–based equalizer.

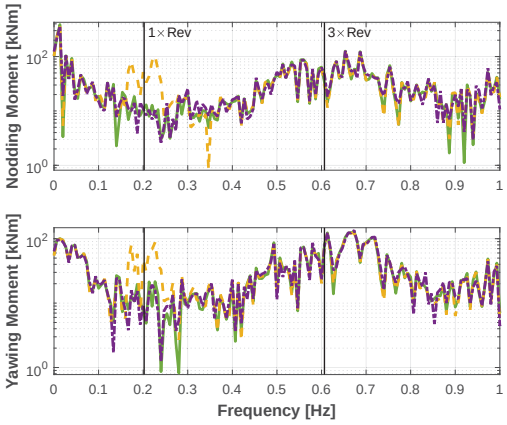

(a)

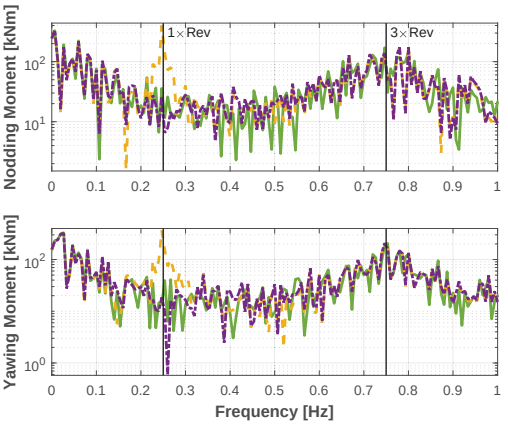

(b)

Figure 5. Comparison of nodding and yawing moments in Cat. A turbulent conditions. Average wind: (a) 7 m/s, (b) 15 m/s. Green solid: no pitch imbalance. Yellow dashed: pitch imbalance, only trimmer. Purple dash–dotted: pitch imbalance, trimmer, MBML–based equalizer.

and target pitch imbalance, while at the same time mitigating shaft loads and consequently blade loads [1,11]. Considering Fig. 2, here all three loops act simultaneously.

In Fig. 6 are reported the yawing and nodding moments on the shaft corresponding to a normal wind profile (NWP) of 15 m/s. No wind conditions in partial power region are considered, for load mitigation via IPC control is generally not adopted in this part of the operating envelope. The green solid line corresponds to a reference condition with no pitch misalignment and a usual Coleman–based cyclic control for load mitigation. The yellow dashed line refers to a condition where the same cyclic control is active but the blades are unbalanced again by 2 deg, 0.5 deg and -0.5 deg respectively. Finally the red dashed–dotted line relates to a case with the same pitch imbalance and where a MBML–based cyclic control for load mitigation and pitch equalization are both active.

By comparing the performance of the Coleman–based cyclic control to the reference – average load values on Fig. 3(b) and Fig. 6 respectively – it is possible to notice a

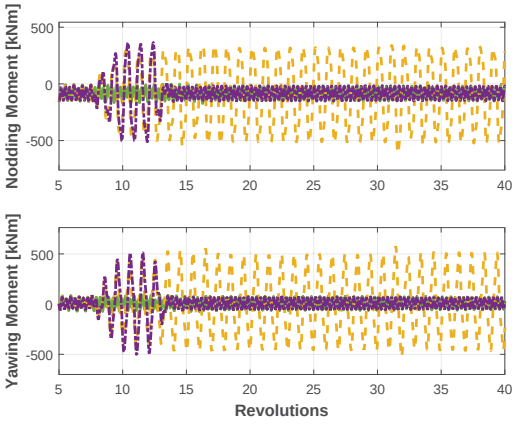

Figure 6. Comparison of nodding and yawing moments in NWP conditions with different controllers for load mitigation at 15 m/s. Green solid: no pitch misalignment, Coleman–based cyclic control. Yellow dashed: pitch misalignment, Coleman–based cyclic control. Purple dash–dotted: pitch misalignment, MBML–based cyclic control and pitch equalizer.

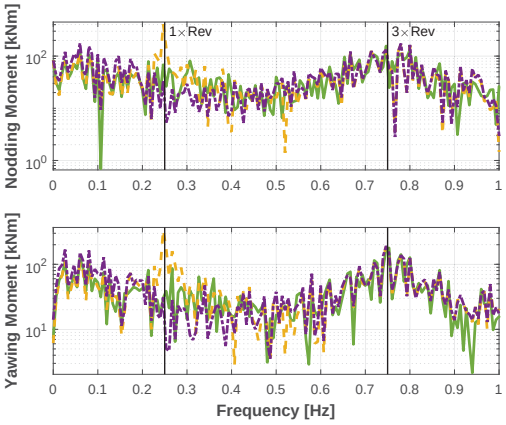

Figure 7. Comparison of nodding and yawing moments in Cat. A turbulent conditions with different controllers for load mitigation at 15 m/s average. Green solid: no pitch misalignment, Coleman–based cyclic control. Yellow dashed: pitch misalignment, Coleman–based cyclic control. Purple dash–dotted: pitch misalignment, MBML–based cyclic control and pitch equalizer.

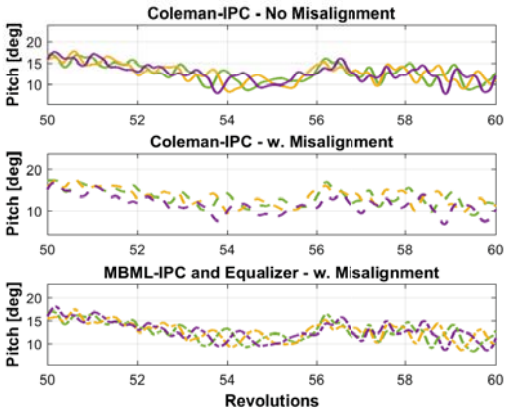

Figure 8. Blade pitches in Cat. A turbulent conditions with different controllers for load mitigation at 15 m/s average. Green, yellow and purple: blade 1, 2 and 3. Top plot, solid lines: no pitch misalignment, Coleman–based cyclic control. Middle plot, dashed: pitch misalignment, Coleman–based cyclic control. Bottom plot, dash–dotted: pitch misalignment, MBML–based cyclic control and pitch equalizer.

good reduction of the average yawing and nodding, as can be expected from this control architecture. On the other hand, when a pitch imbalance is included in the scenario, the performance of the Coleman–based control is unacceptable, with a large increase in the $1 \times$ Rev component. Switching to the MBML transformation both for load mitigation and for pitch equalization, the performance on loads is fully satisfactory even in presence of pitch imbalance, and compares well with the result of usual Bossanyi's control for a balanced rotor.

Similar results are obtained in turbulence, as can be see in Fig. 7 for a Cat. A turbulent wind of 15 m/s. The same three conditions with the same pitch misalignments as in Fig. 6 are considered, but spectra of nodding and yawing are shown instead of time sequences.

It is also interesting to compare the loads of the reference condition (green solid lines, without pitch misalignment) with those obtained when the MBML control is used. In fact, especially around $1 \times$ Rev, the harmonic amplitudes appear lower in the latter case. This is due to the MBML control reacting to any aerodynamic imbalance, including the turbulence–borne one at around $1 \times$ Rev.

Finally, Fig. 8 shows a detail of the time history of the blade pitches for different control scenarios in the same turbulent condition considered for the previous plot. On the top plot, the Coleman–based IPC is working in a condition with null misalignment. The same controller, on the middle plot, is operating in the misaligned condition previously considered. On the bottom plot the proposed MBML–based cyclic and pitch equalizer control are working again in the same misaligned condition. It can be observed that the pitches produced by the MBML–based control in a misaligned condition are very close to those obtained from the standard Coleman–based IPC if no misalignment is present. This demonstrates once again that the control proposed in this work can successfully compensate for a pitch misalignment while keeping the same level of performance obtained from a standard IPC in balanced condition. Furthermore, as expected, from the middle plot, it is possible to verify that the standard IPC, while mitigating cyclic loads, is unable to cope with pitch misalignment.

5 Conclusions

A novel controller for simultaneously targeting aerodynamic imbalances and reducing periodic loads on the rotor has been designed, implemented and tested. Such control algorithm is based on an innovative multi–blade multi–lag transformation, able to fill the lack in performance of the standard Coleman multi–blade transformation.

Based on the results achieved through simulations carried out with a high fidelity model of a 3.0 MW wind turbine, the following conclusions can be derived.

- The proposed MBML transformation is able to measure imbalance–induced biases and periodic blade loads.
- The MBML outputs can be used as feed–back variables to trigger a new control algorithm able to simultaneously target imbalances and mitigate periodic blade loads.
- The proposed algorithm appears as a fully individual pitch control in contrast with the widespread Bossanyi's cyclic.
- As a side effect, the MBML–based control, by mitigating the imbalance–borne load, reduces the source of spurious control action. The actuator duty cycle is therefore reduced.
- The MBML control is capable of mitigating also turbulence–borne imbalances.

An experimental validation of the presented concept is underway. In the meanwhile additional studies shall be related to the evaluation of the effectiveness of the proposed

controller for blade load peak shaving duties. Furthermore, the effects on the stability of the present control is under investigation using an identification–based stability analysis tool [25]. The application of the MBML transformation to active load mitigation for two–bladed rotors will be presented in a forthcoming publication [26].

A Rejection of higher harmonic content of transformed loads via MBML

In this section, we consider the problem of deriving MBML transformations in order to reject higher harmonic content in the transformed loads. To this end, one has to write the harmonic expansion for all blade loads and all lags, as

$$\begin{Bmatrix} \boldsymbol{m}(\psi) \\ \boldsymbol{m}(\psi-\Delta\psi) \\ \vdots \\ \boldsymbol{m}(\psi-L\Delta\psi) \end{Bmatrix} = \begin{bmatrix} \boldsymbol{Q}(\psi) \\ \boldsymbol{Q}(\psi-\Delta\psi) \\ \vdots \\ \boldsymbol{Q}(\psi-L\Delta\psi) \end{bmatrix} \begin{Bmatrix} a_0 \\ a_{1c} \\ a_{1s} \end{Bmatrix} + \boldsymbol{f}. \quad (16)$$

Finally, the unknown harmonic amplitudes can be computed by pseudo–inverting Eq. (16), yielding

$$\begin{Bmatrix} a_0 \\ a_{1_c} \\ a_{1_s} \end{Bmatrix}_{\mathrm{E}} = \frac{1}{L+1} \left[\boldsymbol{C}(\psi) \ \ldots \ \boldsymbol{C}(\psi-L\Delta\psi) \right] \begin{Bmatrix} \boldsymbol{m}(\psi) \\ \boldsymbol{m}(\psi-\Delta\psi) \\ \vdots \\ \boldsymbol{m}(\psi-L\Delta\psi) \end{Bmatrix}, \quad (17)$$

where $\boldsymbol{C}(\psi-\ell\Delta\psi)$ is the standard Coleman transformation evaluated at the ℓth lag angle.

Clearly, Eq. (17) shows that in this specific case, the obtained MBML transformation corresponds to the average among multiple MB transformations at specific lag angles. Specializing Eq. (17) for $L=1$, the following is obtained

$$\begin{Bmatrix} a_0 \\ a_{1_c} \\ a_{1_s} \end{Bmatrix}_{\mathrm{E}} = \frac{1}{2} \left[\boldsymbol{C}(\psi) \ \boldsymbol{C}(\psi-\Delta\psi) \right] \begin{Bmatrix} \boldsymbol{m}(\psi) \\ \boldsymbol{m}(\psi-\Delta\psi) \end{Bmatrix}. \quad (18)$$

Then, expanding each blade moment as in Eq. (1), the estimated amplitudes result to be

$$\begin{Bmatrix} a_0 \\ a_{1_c} \\ a_{1_s} \end{Bmatrix}_{\mathrm{E}} = \frac{1}{2} \begin{Bmatrix} 2a_0 + a_{3c}c_3 + a_{3s}s_3 + f_6 \\ 2a_{1c} + (a_{2c}+a_{4c})\,c_3 + (a_{2s}+a_{4s})\,s_3 + f_6 \\ 2a_{1s} + (a_{4s}-a_{2s})\,c_3 + (a_{2c}-a_{4c})\,s_3 + f_6 \end{Bmatrix}, \quad (19)$$

where $s_3 = \sin(3\psi) - \sin(3(\psi+\Delta\psi))$, $c_3 = \cos(3\psi) - \cos(3(\psi+\Delta\psi))$ and f_6 is a residual at $6\times$Rev depending on the blade load harmonics at $5\times$Rev and higher. Clearly, the utter suppression of $3\times$Rev harmonics is obtained imposing $\cos(3\psi)+\cos(3(\psi-\Delta\psi)) = \sin(3\psi)+\sin(3(\psi-\Delta\psi)) = 0$, a condition satisfied choosing $\Delta\psi = \pi/3$. Hence, the final expression of this MBML transformation matrix is $\frac{1}{2}[\boldsymbol{C}(\psi)\ \boldsymbol{C}(\psi-\pi/3)]$.

Now the twofold benefit of this MBML transformation with respect to the standard MB one appears. Firstly, the residue is at $6\times$Rev, way higher than the one of the standard MB, which is at $3\times$Rev. Secondarily, the absolute value of the residue is really low as it depends on blade harmonics at $5\times$Rev. Conversely, for the standard MB, the residue depends on loads at $2\times$Rev. Both qualities may render the filtering action easier to design, with a lower delay, or even unnecessary. The cost of this transformation is that the support has grown to $\pi/3$.

Following the same procedure, it is also possible to derive MBML transformations with $L \geq 2$. Table 1 describes the characteristics of different MBML transformations, in terms of the number of lags L, the azimuthal sampling $\Delta\psi$, the support s, the frequency content of the residue, the lowest blade harmonic frequency which contributes to the residue and, finally, whether the transformation can be used for bias estimation in order to feed a possible equalizing control law.

Acknowledgments

This research received no specific grant from any funding agency in the public, commercial, or not–for–profit sectors.

References

[1] Bossanyi, E., 2003. "Wind turbine control for load reduction". *Wind Energy*, **6**, pp. 229–244.

[2] Bossanyi, E., 2003. "Individual blade pitch control for load reduction". *Wind Energy*, **6**, pp. 119–128.

[3] Bossanyi, E., 2004. "Developments in individual blade pitch control". In Proceedings of The Science of Making Torque from Wind Conference, Delft, The Netherlands, 19–21 April 2004.

[4] Bossanyi, E., 2005. "Further load reductions with individual pitch control". *Wind Energy*, **8**, pp. 481–485.

[5] Bottasso, C.L., Croce, A., Riboldi, C.E.D., and Nam, Y., 2013. "Multi–layer control architecture for the reduction of deterministic and non–deterministic loads on wind turbines". *Renewable Energy*, **51**, pp. 159–169.

[6] Bottasso, C.L., Croce, A., Riboldi, C.E.D., and Salvetti, M., 2014. "Cyclic pitch control for the reduction of ultimate loads on wind turbines". *Journal Of Physics Conference Series*, **524**(1), 012063.

[7] Geyler, M., and Caselitz, P., 2007. "Individual blade pitch control design for load reduction on large wind turbines". In Proceedings of the European Wind Energy Conference (EWEC 2007), Milano, Italy, 7–10 May 2007.

[8] Leithead, W.E., Neilson, V., and Dominguez, S., 2009. "Alleviation of unbalanced rotor loads by single blade controllers". In Proceedings of the European Wind En-

Table 1. Characteristics of MBML transformations for different lags.

	L	$\Delta\psi$ [deg]	s [deg]	Residual frequency	Lowest blade bearing frequency	Possible bias estimation
$\mathcal{C}_0$ (standard multi-blade)	0	0	0	3×Rev	2×Rev	No
$\mathcal{C}_{1,\pi/3}$	1	60	60	6×Rev	5×Rev	No
$\mathcal{C}_{2,2\pi/9}$	2	40	80	9×Rev	8×Rev	No
$\mathcal{C}_{3,\pi/6}$	3	30	90	12×Rev	11×Rev	No
$\mathcal{C}_{4,2\pi/15}$	4	24	96	15×Rev	14×Rev	No
$\mathcal{C}_{1,2\pi/3}$	1	120	120	3×Rev	2×Rev	Yes
$\mathcal{C}^1_{N-1,2\pi/N}$ (Demodulation)	$N-1$	$360/N$	≈ 360	N×Rev	$(N-1)$×Rev	Yes

ergy Conference (EWEC 2009), Marseille, France, 16–19 March 2009.

[9] Van Engelen, T.G., and Kanev, S., 2009. "Exploring the limits in individual pitch control". In Proceedings of the European Wind Energy Conference (EWEC 2009), Marseille, France, 16–19 March 2009.

[10] Riboldi, C.E.D., 2016. "On the optimal tuning of individual pitch control for horizontal axis wind turbines". *Wind Engineering*, 0309524X16651545.

[11] Riboldi, C.E.D., 2012. "Advanced control laws for variable speed wind turbines and supporting enabling technologies". PhD Thesis, Department of Aerospace Science and Technology, Politecnico di Milano, Italy. See also URL https://www.politesi.polimi.it.

[12] Cacciola, S., Munduate Agud, I., and Bottasso, C.L., 2016. "Detection of rotor imbalance, including root cause, severity and location". *Journal of Physics: Conference Series* **753**, 072003.

[13] Petrović, V., Jelavić, M., and Baotić, M., 2014. "Advanced control algorithms for reduction of wind turbine structural loads". *Renewable Energy* **76**, pp. 418–431.

[14] Bottasso, C.L. and Croce, A., 2006–2012. `Cp-Lambda`: user's manual. Dipartimento di Ingegneria Aerospaziale, Politecnico di Milano, Italy.

[15] Bottasso, C.L., Croce, A., Riboldi, C.E.D., and Nam, Y., 2012. "Power curve tracking in the presence of a tip speed constraint". *Renewable Energy*, **40**, pp. 1–12.

[16] Bottasso, C.L., Croce, A., Savini, B., Sirchi, W., and Trainelli, L., 2005. "Aero–servo elastic modeling and control of wind turbines using finite–element multibody procedures". In Proceedings of the ECCOMAS Multibody Dynamics 2005 Thematic Conference, Madrid, Spain, 21–24 June 2005.

[17] Geyler, M., and Caselitz, P., 2008. "Robust multivariable pitch control design for load reduction on large wind turbines", *Journal of Solar Energy Engineering*, **130**, 031014/1–031014/12.

[18] Many Authors, 2005. "IEC61400–1. Wind turbines – Part 1: design requirements".

[19] Jonkman, J.M., and Buhl, M., 2005. `FAST` User's Guide. National Renewable Energy Laboratory, Boulder, CO.

[20] Stol, K.A., 2003. "Disturbance tracking control and blade load mitigation for variable–speed wind turbines". *ASME Journal of Solar Energy Engineering* **125**, pp. 396–401.

[21] Stol, K.A., and Balas, M.J., 2003. "Periodic disturbance accommodating control for speed regulation of wind turbines". *ASME Journal of Solar Energy Engineering*, **125**, pp. 379–385.

[22] Van Engelen, T.G., 2006. "Design model and load reduction assessment for multi–rotational mode individual pitch control (Higher Harmonics Control)". In Proceedings of the European Wind Energy Conference (EWEC 2006), Athens, Greece, 27 February–2 March 2006.

[23] Bottasso, C.L., Cacciola, S., and Schreiber, J., 2015. "A wake detector for wind farm control". *Journal of Physics: Conference Series*, **625**(1), pp. 012007.

[24] Bauchau, O.A., Bottasso, C.L., and Trainelli, L., 2003. "Robust integration schemes for flexible multibody systems". *Computer Methods in Applied Mechanics and Engineering*, **192**, pp. 395–420.

[25] Bottasso, C.L., and Cacciola, S., 2014. "Model-independent periodic stability analysis of wind turbines". *Wind Energy* **18**(5), pp. 865–887.

[26] Riboldi, C.E.D., and Cacciola, S., 2017. "Individual pitch control for two–bladed wind turbines via multi–blade multi–lag transformation". *Wind Energy*, under review.